

# Supplementary Information for:

## Structure, optical properties, and catalytic applications of alkynyl-protected $M_4Rh_2$ ( $M = Ag/Au$ ) nanoclusters with atomic precision: A comparative study

Leyi Chen,<sup>‡a</sup> Fang Sun,<sup>‡b</sup> Quanli Shen,<sup>a</sup> Lei Wang,<sup>a</sup> Yonggang Liu,<sup>a</sup> Hao Fan,<sup>a</sup> Qing Tang,<sup>b</sup> and Zhenghua Tang<sup>\*a</sup>

<sup>a</sup> *New Energy Research Institute, School of Environment and Energy, South China University of Technology, Guangzhou Higher Education Mega Centre, Guangzhou, 510006, China.*

*\*E-mail: zhht@scut.edu.cn*

<sup>b</sup> *School of Chemistry and Chemical Engineering, Chongqing Key Laboratory of Theoretical and Computational Chemistry, Chongqing University, Chongqing, 401331, China.*

<sup>‡</sup> L. Chen and F. Sun contributed equally to this work.

### List of contents

**Figure S1.** The images of  $Ag_4Rh_2$  and  $Au_4Rh_2$  crystals under an optical microscope.

**Figure S2.** Spatial arrangement of  $Ag_4Rh_2$  in different spatial orientations.

**Figure S3.** Spatial arrangement of  $Au_4Rh_2$  in different spatial orientations.

**Figure S4.** The core-level Ag 3d and Rh 3d XPS spectra of  $Ag_4Rh_2$ .

**Figure S5.** The core-level Au 4f and Rh 3d XPS spectra of  $Au_4Rh_2$ .

**Figure S6.** Time-dependent UV-vis absorption spectra of the conversion of  $Ag_{32}$  to  $Ag_4Rh_2$ .

**Figure S7.** CV curves at different scan rates for  $Ag_4Rh_2$  and  $Au_4Rh_2$ .

**Figure S8.** Stability test of  $Ag_4Rh_2$  and  $Au_4Rh_2$  in HER.

**Figure S9.** Calculated free-energy diagrams for the HER on intact  $Au_4Rh_2$  and  $Ag_4Rh_2$  at zero applied potential.

**Figure S10.** Schematic diagram of the removal of a single alkynyl ligand on  $Au_4Rh_2$  and  $Ag_4Rh_2$ .

**Figure S11.** PDOS of the metal d-states in  $Au_4Rh_2$ ,  $Ag_4Rh_2$ , deligated- $Au_4Rh_2$ , and deligated- $Ag_4Rh_2$ .

**Table S1.** Crystal data and structure refinement for  $Ag_4Rh_2$ .

**Table S2.** Crystal data and structure refinement for  $Au_4Rh_2$ .

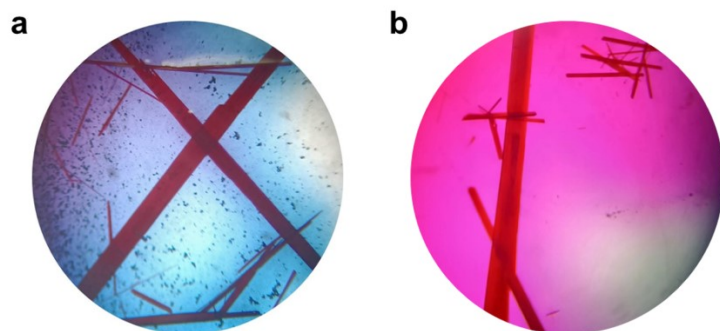


**Figure S1.** The images of (a)  $\text{Ag}_4\text{Rh}_2$  and (b)  $\text{Au}_4\text{Rh}_2$  crystals under an optical microscope.

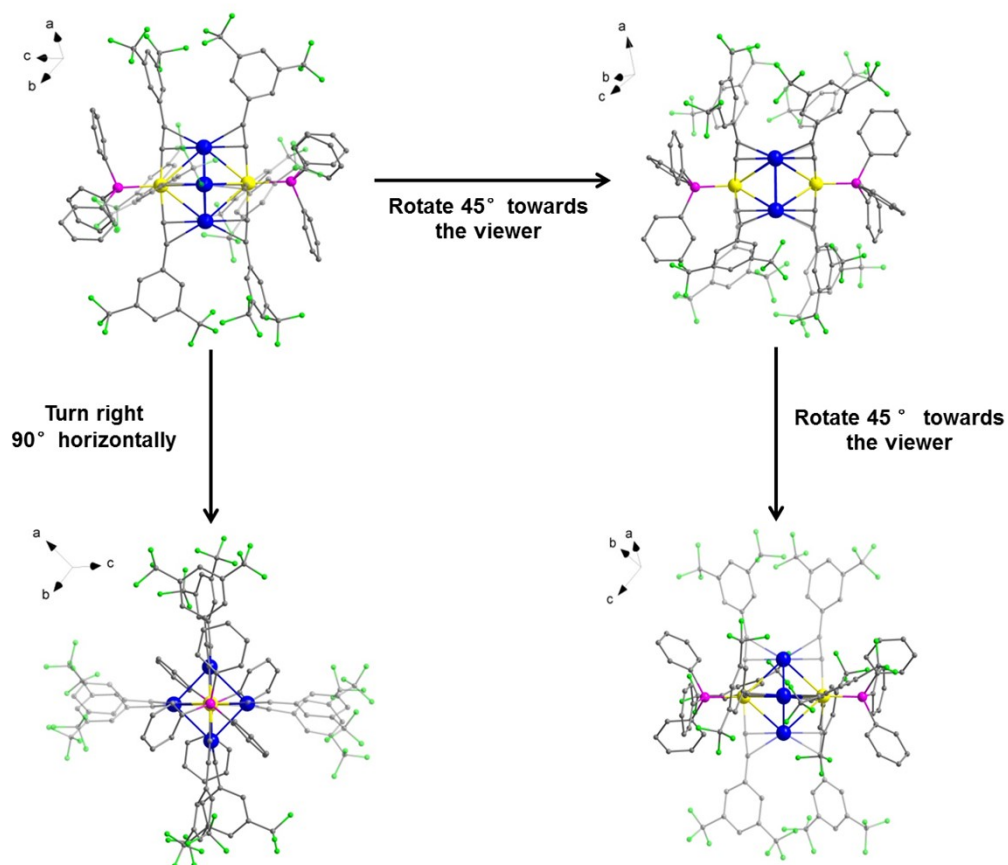


**Figure S2.** Spatial arrangement of  $\text{Ag}_4\text{Rh}_2$  in different spatial orientations. Color code: Ag, blue; Rh, yellow; C, gray; F, green; P, pink. All hydrogen atoms are omitted for clarity.

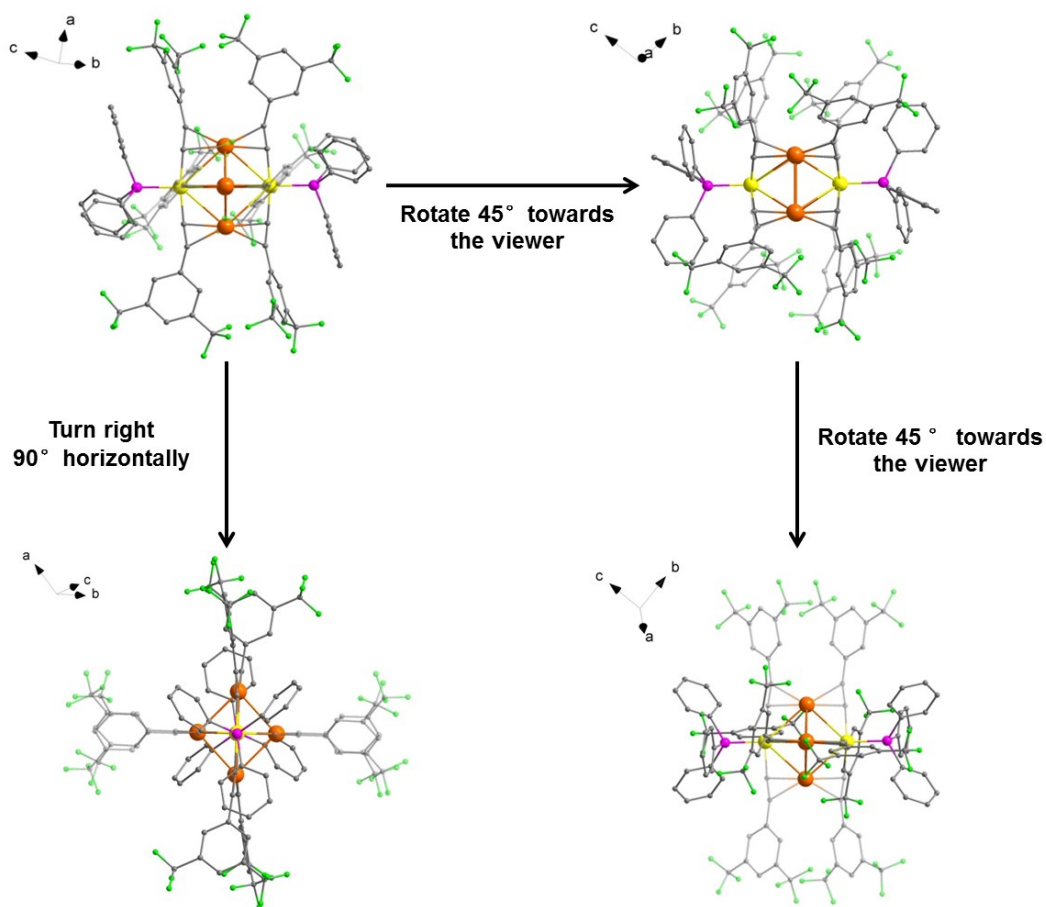


**Figure S3.** Spatial arrangement of  $\text{Au}_4\text{Rh}_2$  in different spatial orientations. Color code: Au, orange; Rh, yellow; C, gray; F, green; P, pink. All hydrogen atoms are omitted for clarity.

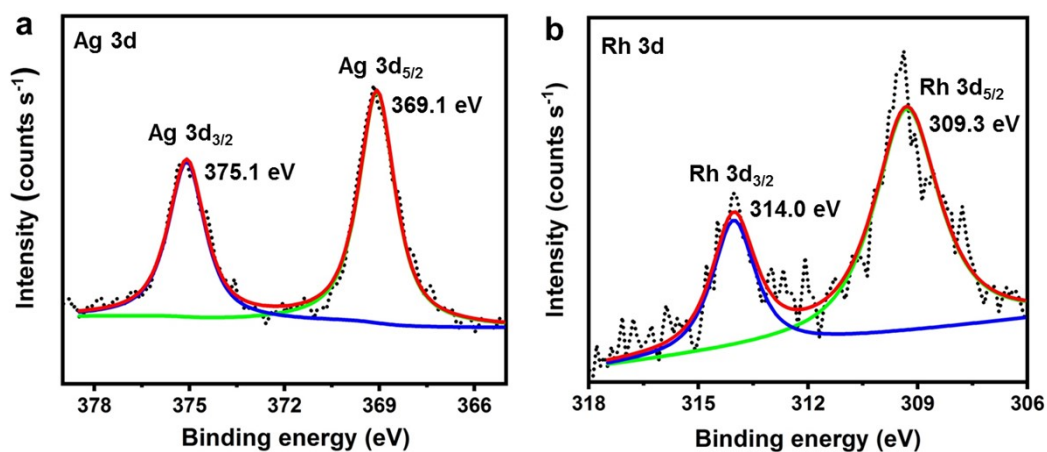


**Figure S4.** The core-level (a) Ag 3d and (b) Rh 3d XPS spectra of  $\text{Ag}_4\text{Rh}_2$ .

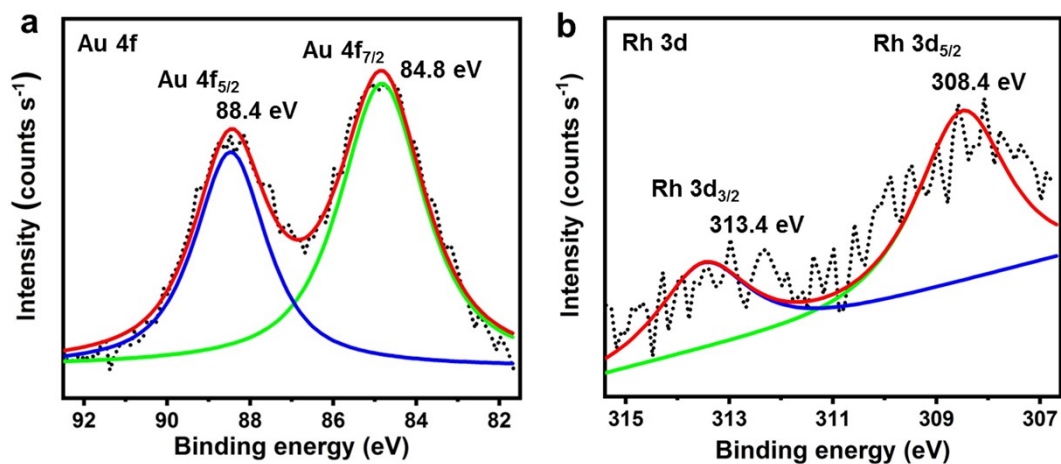


Figure S5. The core-level (a) Au 4f and (b) Rh 3d XPS spectra of Au<sub>4</sub>Rh<sub>2</sub>.

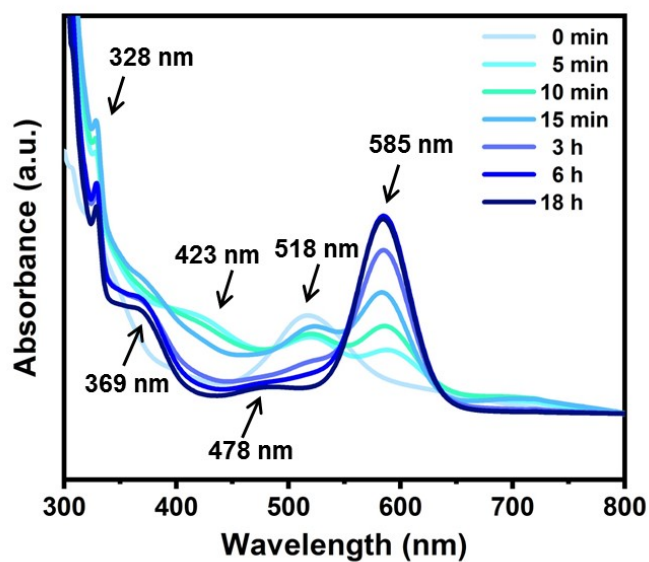
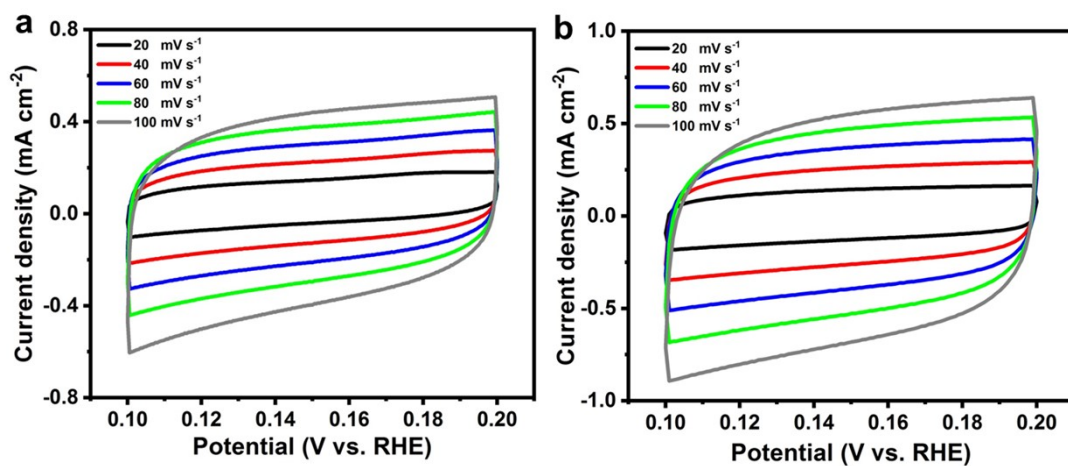
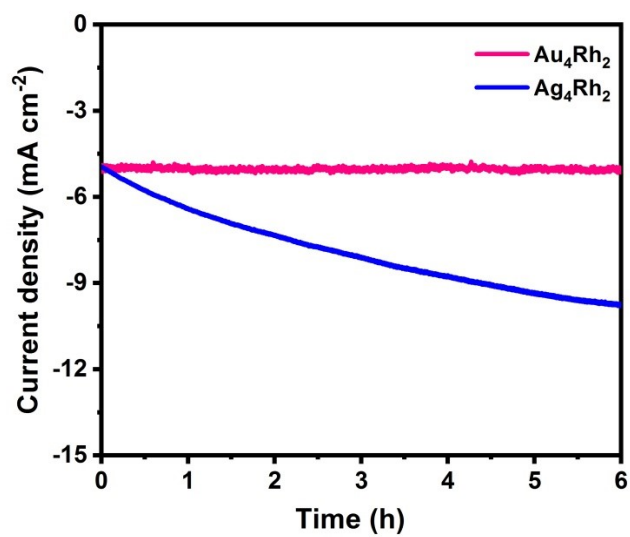


Figure S6. Time-dependent UV-vis absorption spectra of the conversion of Ag<sub>32</sub> to Ag<sub>4</sub>Rh<sub>2</sub>.



**Figure S7.** CV curves at different scan rates (20 to 100  $\text{mV s}^{-1}$ ) for (a)  $\text{Ag}_4\text{Rh}_2$  and (b)  $\text{Au}_4\text{Rh}_2$ .



**Figure S8.** Stability test of  $\text{Ag}_4\text{Rh}_2$  (blue) and  $\text{Au}_4\text{Rh}_2$  (pink) in HER.

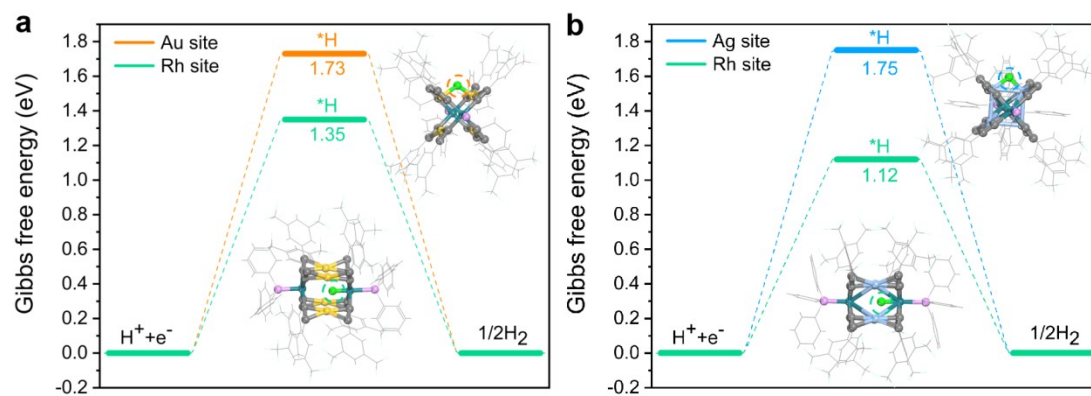


**Figure S9.** Calculated free-energy diagrams for the HER on intact (a)  $\text{Au}_4\text{Rh}_2$  and (b)  $\text{Ag}_4\text{Rh}_2$  at zero applied potential. The inset shows the corresponding optimized structure of a  $^*\text{H}$ -adsorbed. Color code: Au, yellow; Ag, sky blue; Rh, navy blue; P, pink; C, gray; F, cyan; H, white;  $\text{H}^*$ , green. Ligand chains are shown in a linear pattern for clarity.

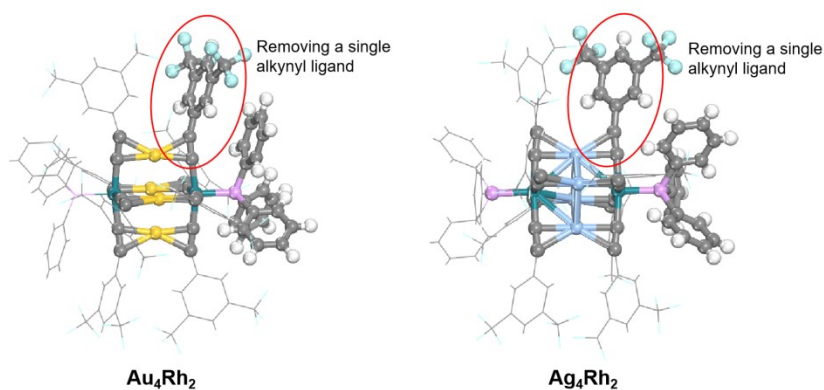


**Figure S10.** The single alkyne ligand for removal on  $\text{Au}_4\text{Rh}_2$  and  $\text{Ag}_4\text{Rh}_2$  is circled in red. Color code: Au, yellow; Ag, sky blue; Rh, navy blue; P, pink; C, gray; F, cyan; H, white.

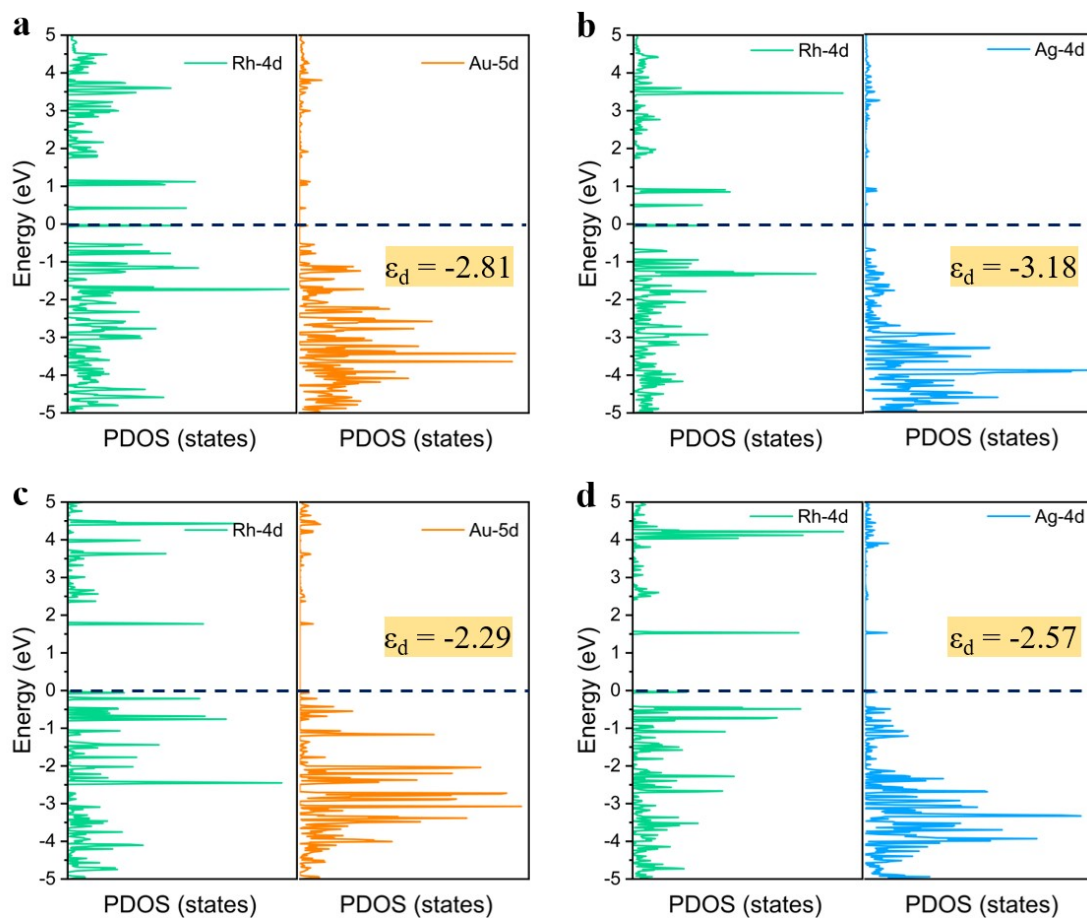


**Figure S11.** PDOS of the metal d-states in (a)  $\text{Au}_4\text{Rh}_2$ , (b)  $\text{Ag}_4\text{Rh}_2$ , (c) deligated- $\text{Au}_4\text{Rh}_2$ , and (d) deligated- $\text{Ag}_4\text{Rh}_2$  clusters. Of note, the Fermi energy levels have been normalized to zero (black dotted line).

**Table S1.** Crystal data and structure refinement for Ag<sub>4</sub>Rh<sub>2</sub>.

Chemical formula	C <sub>116</sub> H <sub>54</sub> Ag <sub>4</sub> F <sub>48</sub> P <sub>2</sub> Rh <sub>2</sub>
Formula weight	6585.32
Temperature/K	149.99(10)
Crystal system	monoclinic
Space group	<i>P2<sub>1</sub>/n</i>
<i>a</i> /Å	27.0491(3)
<i>b</i> /Å	29.5409(3)
<i>c</i> /Å	34.5184(4)
$\alpha$ /°	90.0
$\beta$ /°	111.6840(10)
$\gamma$ /°	90.0
<i>V</i> /Å <sup>3</sup>	25630.3(5)
<i>Z</i>	4
$\rho_{\text{calc}}$ /cm <sup>3</sup>	1.707
$\mu$ /mm <sup>-1</sup>	8.157
F(000)	12932
Crystal size/mm <sup>3</sup>	0.70 × 0.10 × 0.08
Radiation	Cu K $\alpha$ ( $\lambda$ = 1.54178)
2 $\theta$ range for data collection/°	6.006 to 148.604
Index ranges	-33 ≤ <i>h</i> ≤ 23, -36 ≤ <i>k</i> ≤ 36, -42 ≤ <i>l</i> ≤ 42
Reflections collected	108374
Independent reflections	50559 [ <i>R</i> <sub>int</sub> = 0.0455, <i>R</i> <sub>sigma</sub> = 0.0625]
Data/restraints/parameters	50559/8282/3624
Goodness-of-fit on <i>F</i> <sup>2</sup>	1.032
Final <i>R</i> indexes [ <i>I</i> ≥ 2 $\sigma$ ( <i>I</i> )]	<i>R</i> <sub>1</sub> = 0.0730, <i>wR</i> <sub>2</sub> = 0.1707
Final <i>R</i> indexes [all data]	<i>R</i> <sub>1</sub> = 0.1053, <i>wR</i> <sub>2</sub> = 0.1984
Largest diff. peak/hole/e Å <sup>-3</sup>	2.070/ -1.573



**Table S2.** Crystal data and structure refinement for Au<sub>4</sub>Rh<sub>2</sub>.

Chemical formula	C <sub>116</sub> H <sub>54</sub> Au <sub>4</sub> F <sub>48</sub> P <sub>2</sub> Rh <sub>2</sub>
Formula weight	3691.62
Temperature/K	120(2)
Crystal system	triclinic
Space group	<i>P</i> 1
<i>a</i> /Å	17.16177(18)
<i>b</i> /Å	17.24053(19)
<i>c</i> /Å	24.4066(2)
$\alpha$ /°	90.3557(8)
$\beta$ /°	103.8441(8)
$\gamma$ /°	115.4022(10)
<i>V</i> /Å <sup>3</sup>	6284.73(12)
<i>Z</i>	2
$\rho_{\text{calc}}$ /cm <sup>3</sup>	1.951
$\mu$ /mm <sup>-1</sup>	5.057
F(000)	3536
Crystal size/mm <sup>3</sup>	0.10 × 0.03 × 0.03
Radiation	Mo K $\alpha$ ( $\lambda$ = 0.71073)
2 $\theta$ range for data collection/°	4.482 to 62.050
Index ranges	-24 ≤ <i>h</i> ≤ 24, -24 ≤ <i>k</i> ≤ 23, -33 ≤ <i>l</i> ≤ 34
Reflections collected	183311
Independent reflections	33635 [ <i>R</i> <sub>int</sub> = 0.0541, <i>R</i> <sub>sigma</sub> = 0.0469]
Data/restraints/parameters	33635/2284/2053
Goodness-of-fit on <i>F</i> <sup>2</sup>	1.033
Final <i>R</i> indexes [ <i>I</i> ≥ 2 $\sigma$ ( <i>I</i> )]	<i>R</i> <sub>1</sub> = 0.0378, <i>wR</i> <sub>2</sub> = 0.0868
Final <i>R</i> indexes [all data]	<i>R</i> <sub>1</sub> = 0.0604, <i>wR</i> <sub>2</sub> = 0.0951
Largest diff. peak/hole/e Å <sup>-3</sup>	1.872/-2.887